
No Training, No Problem: Rethinking Classifier-Free Guidance for Diffusion Models

Seyedmorteza Sadat¹, Manuel Kansy¹, Otmar Hilliges¹, Romann M. Weber²

¹ETH Zürich, ²DisneyResearchStudios

{seyedmorteza.sadat, manuel.kansy, otmar.hilliges}@inf.ethz.ch
{romann.weber}@disneyresearch.com

Abstract

Classifier-free guidance (CFG) has become the standard method for enhancing the quality of conditional diffusion models. However, employing CFG requires either training an unconditional model alongside the main diffusion model or modifying the training procedure by periodically inserting a null condition. There is also no clear extension of CFG to unconditional models. In this paper, we revisit the core principles of CFG and introduce a new method, independent condition guidance (ICG), which provides the benefits of CFG without the need for any special training procedures. Our approach streamlines the training process of conditional diffusion models and can also be applied during inference on any pre-trained conditional model. Additionally, by leveraging the time-step information encoded in all diffusion networks, we propose an extension of CFG, called time-step guidance (TSG), which can be applied to *any* diffusion model, including unconditional ones. Our guidance techniques are easy to implement and have the same sampling cost as CFG. Through extensive experiments, we demonstrate that ICG matches the performance of standard CFG across various conditional diffusion models. Moreover, we show that TSG improves generation quality in a manner similar to CFG, without relying on any conditional information.

1 Introduction

Diffusion models have recently emerged as the main methodology behind many successful generative models [39, 14, 9, 33, 42, 43]. At the core of such models lies a diffusion process that gradually adds noise to the data until data points are indistinguishable from pure noise. At inference, a denoiser is used to gradually remove noise from samples until we reach a generated data point. While the theory suggests that standard sampling from diffusion models should yield high-quality images, this does not generally hold in practice, and guidance methods are often required to increase the quality of generations, albeit at the expense of less diversity [9, 13, 35]. Classifier guidance [9] was the first method to introduce this concept by utilizing the gradient of a classifier trained on noisy images to increase the class-likelihood of generated samples. Later, classifier-free guidance (CFG) [13] was proposed, allowing the diffusion model to simulate the same behavior as classifier guidance without using an explicit classifier. Since then, CFG has been applied to other conditional generation tasks, such as text-to-image synthesis [28] and text-to-3D generation [31].

In addition to CFG’s trading diversity for quality, it has two practical limitations. First, it requires the underlying model to be trained in a specific way to also learn the unconditional score function, typically by replacing the conditioning vector with a null vector with probability p (usually $p \in [0.1, 0.2]$). This additional step hinders training efficiency, as the model needs to be trained on two different tasks. Replacing the condition might also not be straightforward when the model is multimodal and uses different conditioning signals such as text, images, and audio at the same time, or when the null vector (which is usually the zero vector in practice) has a specific meaning. Second,

it is not clear how to extend the benefits of classifier-free guidance beyond conditional models to unconditional generation.

In this paper, we analyze the methodology behind classifier-free guidance and show theoretically that similar behavior can be achieved without additional training of an unconditional model. The main idea is that by using a conditioning vector independent of the input data, the conditional score function becomes equivalent to the unconditional score. This insight leads us to propose *independent condition guidance* (ICG), a method that replicates the behavior of CFG at inference time without requiring separate training of an unconditional model.

Inspired by the above, we also introduce a novel technique to extend classifier-free guidance to a more general setting that includes unconditional generation. This method, which we call *time-step guidance* (TSG), employs a perturbed version of the time-step embedding in diffusion models to create a guidance signal similar to CFG. Time-step guidance aims to improve the accuracy of denoising at each sampling step by leveraging the time-step information learned by the diffusion model to steer sampling trajectories toward better noise-removal paths.

Our guidance techniques are easy to implement, do not require additional fine-tuning of the underlying diffusion models, and have the same sampling cost as CFG. Through extensive experiments, we empirically verify that: 1) ICG offers performance similar to CFG and can be readily applied to models that are not trained with the CFG objective in mind, such as EDM [18]; and 2) TSG improves output quality in a manner similar to CFG for both conditional and unconditional generation.

The core contributions of our work are as follows: (i) We revisit the principles of classifier-free guidance and offer an efficient, theoretically motivated method to employ CFG without the need to train an unconditional module, greatly simplifying the training process of conditional diffusion models. (ii) We offer an extension of CFG that is generally applicable to all diffusion models, whether conditional or unconditional. (iii) We demonstrate empirically that our guidance techniques achieve the quality-boosting benefits of CFG across various setups and network architectures.

2 Related work

Score-based diffusion models [42, 43, 39, 14] learn the data distribution by reversing a forward diffusion process that progressively transforms the data into Gaussian noise. These models have quickly surpassed the fidelity and diversity of previous generative modeling methods [27, 9], achieving state-of-the-art results in various domains, including unconditional image generation [9, 18], text-to-image generation [32, 37, 2, 33, 30, 47], video generation [5, 4, 10], image-to-image translation [36, 22], motion synthesis [45, 46], and audio generation [7, 20, 17].

Since the development of the DDPM model [14], many advancements have been proposed including improved network architectures [16, 19, 29, 9], sampling algorithms [40, 18, 23, 24, 38], and training methods [27, 18, 43, 38, 33]. Despite these recent advances, diffusion guidance, including classifier [9] and classifier-free guidance [13], still plays an essential role in improving the quality of generations as well as increasing the alignment between the condition and the output image [28].

SAG [15] and PAG [1] have recently been proposed to increase the quality of UNet-based diffusion models by modifying the predictions of the self-attention layers. Our method is complementary to these approaches, as one can combine ICG updates with the update signal from the perturbed attention modules [15]. In addition, we make no assumptions about the network architecture.

Another line of work includes guiding the generation of the diffusion model with a differentiable loss function or an off-the-shelf classifier [41, 8, 48, 3, 11]. These methods are primarily focused on solving inverse problems, typically with unconditional models, while we are instead concerned with achieving the benefits of CFG in conditional models without any additional training requirements. With TSG, we also generalize our approach to extend CFG-like benefits to unconditional models.

Perturbing the condition vector is employed in CADs [35] to increase the diversity of generations. CADs differs from ICG in focusing on the *conditional* branch to improve diversity, while ICG is concerned with the *unconditional* branch to simulate CFG. Since CADs is designed to enhance the diversity of CFG, it can be used alongside ICG to improve the diversity of output at high guidance scales (see Appendix C.1).

3 Background

This section provides an overview of diffusion models. Let $\mathbf{x} \sim p_{\text{data}}(\mathbf{x})$ be a data point, $t \in [0, 1]$ be the time step, and $\mathbf{z}_t = \mathbf{x} + \sigma(t)\epsilon$ be the forward process of the diffusion model that adds noise to the data. Here $\sigma(t)$ is the noise schedule and determines how much information is destroyed at each time step t , with $\sigma(0) = 0$ and $\sigma(1) = \sigma_{\text{max}}$. Karras et al. [18] showed that this forward process corresponds to the ordinary differential equation (ODE)

$$d\mathbf{z} = -\dot{\sigma}(t)\sigma(t) \nabla_{\mathbf{z}_t} \log p_t(\mathbf{z}_t) dt \quad (1)$$

or, equivalently, a stochastic differential equation (SDE) given by

$$d\mathbf{z} = -\dot{\sigma}(t)\sigma(t) \nabla_{\mathbf{z}_t} \log p_t(\mathbf{z}_t) dt - \beta(t)\sigma(t)^2 \nabla_{\mathbf{z}_t} \log p_t(\mathbf{z}_t) dt + \sqrt{2\beta(t)}\sigma(t) d\omega_t. \quad (2)$$

Here $d\omega_t$ is the standard Wiener process, and $p_t(\mathbf{z}_t)$ is the time-dependent distribution of noisy samples, with $p_0 = p_{\text{data}}$ and $p_1 = \mathcal{N}(\mathbf{0}, \sigma_{\text{max}}^2 \mathbf{I})$. Assuming that we have access to the time-dependent score function $\nabla_{\mathbf{z}_t} \log p_t(\mathbf{z}_t)$, we can sample from the data distribution p_{data} by solving the ODE or SDE backward in time (from $t = 1$ to $t = 0$). The unknown score function $\nabla_{\mathbf{z}_t} \log p_t(\mathbf{z}_t)$ is estimated via a neural denoiser $D_{\theta}(\mathbf{z}_t, t)$ that is trained to predict the clean samples \mathbf{x} from the corresponding noisy samples \mathbf{z}_t . The framework allows for conditional generation by training a denoiser $D_{\theta}(\mathbf{z}_t, t, \mathbf{y})$ that accepts additional input signals \mathbf{y} , such as class labels or text prompts.

Training objective Given a noisy sample \mathbf{z}_t at time step t , the denoiser $D_{\theta}(\mathbf{z}_t, t, \mathbf{y})$ with parameters θ can be trained with the standard MSE loss (also called denoising score matching loss)

$$\arg \min_{\theta} \mathbb{E}_t \left[\|D_{\theta}(\mathbf{z}_t, t, \mathbf{y}) - \mathbf{x}\|^2 \right]. \quad (3)$$

The trained denoiser approximates the time-dependent conditional score function $\nabla_{\mathbf{z}_t} \log p_t(\mathbf{z}_t | \mathbf{y})$ via

$$\nabla_{\mathbf{z}_t} \log p_t(\mathbf{z}_t | \mathbf{y}) \approx \frac{D_{\theta}(\mathbf{z}_t, t, \mathbf{y}) - \mathbf{z}_t}{\sigma(t)^2}. \quad (4)$$

Classifier-free guidance (CFG) CFG is an inference method for improving the quality of generated outputs by mixing the predictions of a conditional and an unconditional model [13]. Specifically, given a null condition $\mathbf{y}_{\text{null}} = \emptyset$ corresponding to the unconditional case, CFG modifies the output of the denoiser at each sampling step according to

$$\hat{D}_{\theta}(\mathbf{z}_t, t, \mathbf{y}) = D_{\theta}(\mathbf{z}_t, t, \mathbf{y}_{\text{null}}) + w_{\text{CFG}}(D_{\theta}(\mathbf{z}_t, t, \mathbf{y}) - D_{\theta}(\mathbf{z}_t, t, \mathbf{y}_{\text{null}})), \quad (5)$$

where $w_{\text{CFG}} = 1$ corresponds to the non-guided case. The unconditional model $D_{\theta}(\mathbf{z}_t, t, \mathbf{y}_{\text{null}})$ is trained by randomly assigning the null condition $\mathbf{y}_{\text{null}} = \emptyset$ to the input of the denoiser with probability p , where we normally have $p \in [0.1, 0.2]$. One can also train a separate denoiser to estimate the unconditional score in Equation (5) [19]. Similar to the truncation method in GANs [6], CFG increases the quality of individual images at the expense of less diversity [26].

4 Revisiting classifier-free guidance

We now show how a conditional model can be used to simulate the behavior of classifier-free guidance, without the need to train an extra unconditional model. The analysis in this section is inspired by Sadat et al. [35].

First, note that at each time step t , classifier-free guidance uses the conditional score $\nabla_{\mathbf{z}_t} \log p_t(\mathbf{z}_t | \mathbf{y})$ and the unconditional score $\nabla_{\mathbf{z}_t} \log p_t(\mathbf{z}_t)$ to guide the sampling process. Based on Bayes' theorem, we can write $p_t(\mathbf{z}_t | \mathbf{y}) = \frac{p_t(\mathbf{y} | \mathbf{z}_t) p_t(\mathbf{z}_t)}{p_t(\mathbf{y})}$, which gives us

$$\nabla_{\mathbf{z}_t} \log p_t(\mathbf{z}_t | \mathbf{y}) = \nabla_{\mathbf{z}_t} \log p_t(\mathbf{z}_t) + \nabla_{\mathbf{z}_t} \log p_t(\mathbf{y} | \mathbf{z}_t). \quad (6)$$

Next, assume that we replace the condition with a random vector $\hat{\mathbf{y}}$ that is independent of the input \mathbf{z}_t . In this case, we have $p_t(\hat{\mathbf{y}} | \mathbf{z}_t) = p_t(\hat{\mathbf{y}})$, which gives us

$$\nabla_{\mathbf{z}_t} \log p_t(\mathbf{z}_t | \hat{\mathbf{y}}) = \nabla_{\mathbf{z}_t} \log p_t(\mathbf{z}_t) + \nabla_{\mathbf{z}_t} \log p_t(\hat{\mathbf{y}}) = \nabla_{\mathbf{z}_t} \log p_t(\mathbf{z}_t). \quad (7)$$

This analysis shows that we can estimate the unconditional score purely based on the conditional model by replacing the condition \mathbf{y} with an independent vector $\hat{\mathbf{y}}$. Based on this derivation, we argue that there is no need to train a separate model $D_{\theta}(\mathbf{z}_t, t, \mathbf{y}_{\text{null}})$ for applying classifier-free guidance as we can use the conditional model itself to bootstrap the score of the unconditional distribution as long as we pick an input condition that is independent of \mathbf{z}_t . We call this method *independent condition guidance* (ICG) for the rest of the paper.

The intuition behind ICG becomes more clear in the class-conditional case. Notice that by knowing the conditional distribution $p_t(\mathbf{z}_t | \mathbf{y})$ for each \mathbf{y} , we also implicitly obtain the unconditional distribution through $p_t(\mathbf{z}_t) = \sum_{\mathbf{y}} p_t(\mathbf{z}_t | \mathbf{y}) p(\mathbf{y})$. The major limitation of directly applying this formula is the necessity for multiple forward passes (one for each class). ICG circumvents this issue by deriving the unconditional score efficiently from the conditional model using only a single forward pass through the network. Thus, the sampling cost of ICG is equal to that of standard CFG.

Implementation details Although the analysis above holds for any condition $\hat{\mathbf{y}}$ that is independent of \mathbf{z}_t , an appropriate $\hat{\mathbf{y}}$ must be selected for the model input in practice. We experiment with two options for the independent condition. First, $\hat{\mathbf{y}}$ can be drawn from a Gaussian distribution with a suitable standard deviation so that $\hat{\mathbf{y}}$ matches the scale of the actual conditioning vector \mathbf{y} . Second, a random condition from the conditioning space, such as a random class label or random clip tokens, can be chosen as the independent $\hat{\mathbf{y}}$. We show in Section 7 that both methods perform similarly. However, there may be a slight preference for the random condition over Gaussian noise, as it stays closer to the conditioning distribution that the diffusion model was trained on.

5 Time-step guidance

Inspired by ICG, we next offer an extension of classifier-free guidance that can be used with any model, including unconditional networks. We begin our analysis with class-conditional models and subsequently extend it to a more general setting.

In the class-conditional case, the embedding vector of the class is typically added to the embedding vector of the time step t to compute the input condition of the diffusion network. Hence, in practice, CFG essentially uses the outputs of the diffusion network for two different input embeddings and takes their difference as the update direction. Thus, we might directly utilize the time-step embedding of each diffusion model as a means to define a similar guidance signal. This leads to a novel method that we refer to as *time-step guidance* (TSG), which, like CFG, increases the quality of generations but, unlike CFG, is applicable even to unconditional models.

In this method, we compute the model outputs for the clean time-step embedding and a perturbed embedding and use their difference to guide the sampling. More specifically, at each time step t , we update the output via

$$\hat{D}_{\theta}(\mathbf{z}_t, t) = D_{\theta}(\mathbf{z}_t, \tilde{t}) + w_{\text{TSG}}(D_{\theta}(\mathbf{z}_t, t) - D_{\theta}(\mathbf{z}_t, \tilde{t})), \quad (8)$$

where \tilde{t} is the perturbed version of t . The intuition behind TSG is that at each time step t , altering the time-step embedding of the network leads to denoised outputs with either insufficient or excessive noise removal (see Figure 7 in the appendix). Consequently, these outputs can be exploited to prevent the network from going toward undesirable predictions, thus increasing the accuracy of the score predictions at each time step. As we show below, TSG is related to stochastic Langevin dynamics in terms of the first-order approximation, and hence, is expected to improve generation quality.

Connection to Langevin dynamics Let $\tilde{t} = t + \Delta t$, where Δt is a small perturbation. Using a Taylor expansion, we get $D_{\theta}(\mathbf{z}_t, \tilde{t}) = D_{\theta}(\mathbf{z}_t, t) + \frac{\partial D_{\theta}(\mathbf{z}_t, t)}{\partial t} \Delta t$. Hence, $\hat{D}_{\theta}(\mathbf{z}_t, \tilde{t}) = D_{\theta}(\mathbf{z}_t, t) + (1 - w_{\text{TSG}}) \frac{\partial D_{\theta}(\mathbf{z}_t, t)}{\partial t} \Delta t$. Based on Equation (4), the score function is equal to

$$\nabla_{\mathbf{z}_t} \log \hat{p}_t(\mathbf{z}_t) = \nabla_{\mathbf{z}_t} \log p_t(\mathbf{z}_t) + \frac{1 - w_{\text{TSG}}}{\sigma(t)^2} \frac{\partial D_{\theta}(\mathbf{z}_t, t)}{\partial t} \Delta t. \quad (9)$$

Now, if we follow the Euler sampling step for solving Equation (1), i.e. we define the update rule as $\mathbf{z}_{t-1} = \mathbf{z}_t + \eta_t \nabla_{\mathbf{z}_t} \log \hat{p}_t(\mathbf{z}_t)$, then the modified sampling step after time-step guidance will be equal to

$$\mathbf{z}_{t-1} = \mathbf{z}_t + \eta_t \nabla_{\mathbf{z}_t} \log p_t(\mathbf{z}_t) + \eta_t \frac{1 - w_{\text{TSG}}}{\sigma(t)^2} \frac{\partial D_{\theta}(\mathbf{z}_t, t)}{\partial t} \Delta t. \quad (10)$$

Assuming that Δt is a Gaussian random variable with zero mean, the update rule resembles a Langevin dynamics step, where the noise strength is determined based on the network behavior as represented by $\frac{\partial D_{\theta}(z_t, t)}{\partial t}$. As Langevin dynamics is known to increase the quality of sampling from a given distribution by compensating for the errors happening at each sampling step, we argue that TSG also behaves similarly in terms of first-order approximation.

Implementation details In practice, we implement TSG by perturbing the time-step embedding with zero-mean Gaussian noise according to $\tilde{t}_{\text{emb}} = t_{\text{emb}} + st^{\alpha}\mathbf{n}$ where $\mathbf{n} \sim \mathcal{N}(\mathbf{0}, \mathbf{I})$ and st^{α} determines the noise scale at each time step t . We choose s and α such that the scale of the noise portion becomes comparable to the scale of the time-step embedding t_{emb} . Empirically, we also find that it is sometimes beneficial to apply the perturbed embeddings only to a portion of layers in the diffusion network, e.g., using \tilde{t}_{emb} for the first 10 layers and t_{emb} for the rest of layers. We provide ablations on these hyperparameters in Section 7.

6 Experiments

In this section, we rigorously evaluate ICG and demonstrate its ability to simulate the behavior of CFG across several conditional models. Additionally, we show that TSG improves the quality of both conditional and unconditional generations compared to the non-guided sampling baseline.

Setup All experiments are conducted via pre-trained checkpoints provided by official implementations. We use the recommended sampler that comes with each model, such as the EDM sampler for EDM networks [18], DPM++ [25] for Stable Diffusion [33], and DDPM [14] for DiT-XL/2 [29].

Evaluation We use Fréchet Inception Distance (FID) [12] as the main metric to measure both quality and diversity due to its alignment with human judgment. As FID is known to be sensitive to small implementation details, we ensure that models under comparison follow the same evaluation setup. For completeness, we also report precision [21] as a standalone quality metric and recall [21] as a diversity metric whenever possible. $\text{FD}_{\text{DINOv2}}$ [44] is also reported for the EDM2 model [19].

6.1 Comparison between ICG and CFG

Qualitative results The qualitative comparisons between ICG and CFG are given in Figure 1 for Stable Diffusion [33] and DiT-XL/2 [29] models. Figure 2 also shows a comparison between the EDM2 model [19] guided with a separate unconditional module vs ICG. We observe that both ICG and CFG improve image quality, and the ICG and CFG outputs are almost identical. This empirical evidence agrees with our theoretical justification provided in Section 4.

Quantitative results We now show that ICG and CFG both result in similar performance metrics across several conditional models. As shown in Table 1, compared to CFG, ICG achieves better or similar performance across all metrics.¹ In Table 2, we also compare the effect of ICG on EDM [18] and EDM2 [19] models that were not trained with the CFG objective. The table shows that ICG performs similarly to guiding the generations with a separate unconditional module.

Varying the Guidance Scale Next, we demonstrate that by varying the guidance scale of ICG, we can increase the quality of outputs in a manner similar to standard CFG. As shown in Figure 3, increasing the guidance scale improves precision but reduces recall. The FID plots also form a U-shaped curve, consistent with what we expect from standard CFG.

6.2 Results for ControlNet

We also show that ICG can be used for improving the quality of image-conditioned models as well. We use ControlNet as an example in this section since it is not trained with the CFG objective on the image condition input. That is, it only applies CFG to the text component of the condition. Our results are given in Figure 4. We see that without any text prompt, ICG significantly improves the quality of generations over the base sampling.

¹For MDM, the recall metric is not available, and R-precision is reported similarly to the original paper [45].

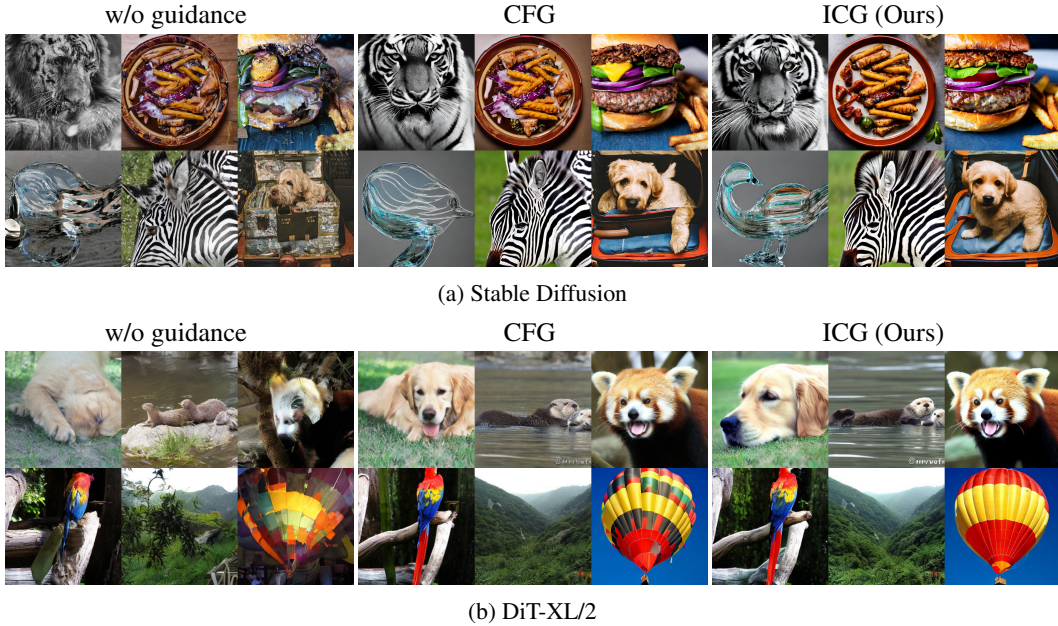


Figure 1: Comparison between CFG and ICG for (a) Stable Diffusion [33] and (b) DiT-XL/2 [29]. Both CFG and ICG significantly improve the image quality of the baseline. Also note the similarity between the outputs of CFG and ICG, confirming our theoretical analysis in Section 4.



Figure 2: Comparison between the EDM2 model [19] guided with another unconditional module and ICG. We observe that using ICG leads to similar generations as CFG, and both methods significantly improve output quality compared to sampling without guidance.

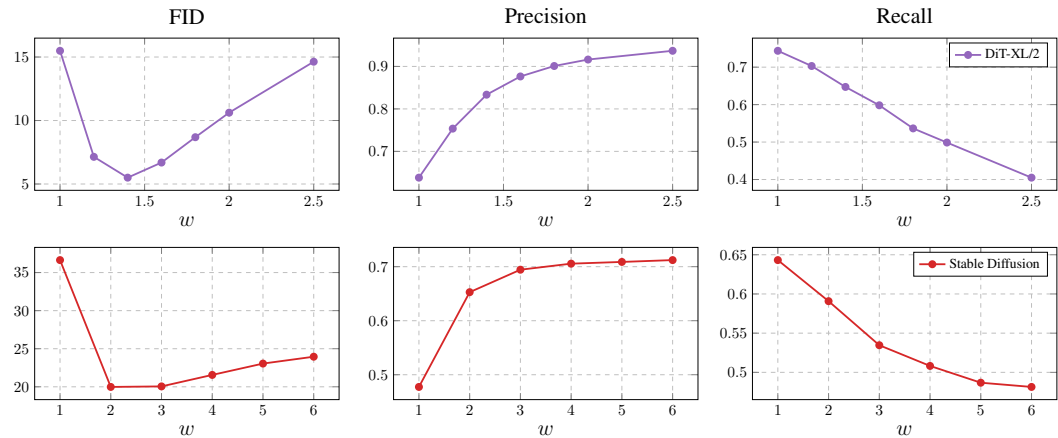


Figure 3: Comparison between different metrics as the guidance scale increases. Similar to CFG, ICG trades diversity (lower recall) with quality (higher precision) as the guidance scale increases.

Table 1: Quantitative comparison between CFG and ICG. ICG is able to achieve similar metrics to the standard CFG by extracting the unconditional score from the conditional model itself.

Model	Architecture	Guidance	FID ↓	Precision ↑	Recall ↑
Stable Diffusion [33]	UNet	CFG	20.13	0.69	0.54
		ICG (Ours)	20.05	0.69	0.53
DiT-XL/2 [29]	Transformer	CFG	5.56	0.81	0.66
		ICG (Ours)	5.50	0.83	0.65
Pose-to-Image [35]	UNet	CFG	14.61	0.93	0.02
		ICG (Ours)	13.46	0.94	0.03
MDM [45]	Transformer	CFG	0.65	0.73	-
		ICG (Ours)	0.47	0.71	-

Table 2: Quantitative comparison between CFG and ICG for EDM networks. Although these models are not trained with the CFG objective, guiding their generations using a separate unconditional module results in similar outcomes to using ICG.

Model	Dataset	Guidance	FID ↓	FD _{DINOv2} ↓
EDM2-XS [19]	Imagenet	CFG	3.36	79.94
		ICG (Ours)	3.35	79.54
EDM [18]	CIFAR-10	CFG	1.87	-
		ICG (Ours)	1.87	-



(a) Pose-to-image generation



(b) Depth-to-image generation

Figure 4: Image-conditioned generation with ControlNet (without prompt). ICG significantly increases the quality of generations by applying guidance to the image condition.

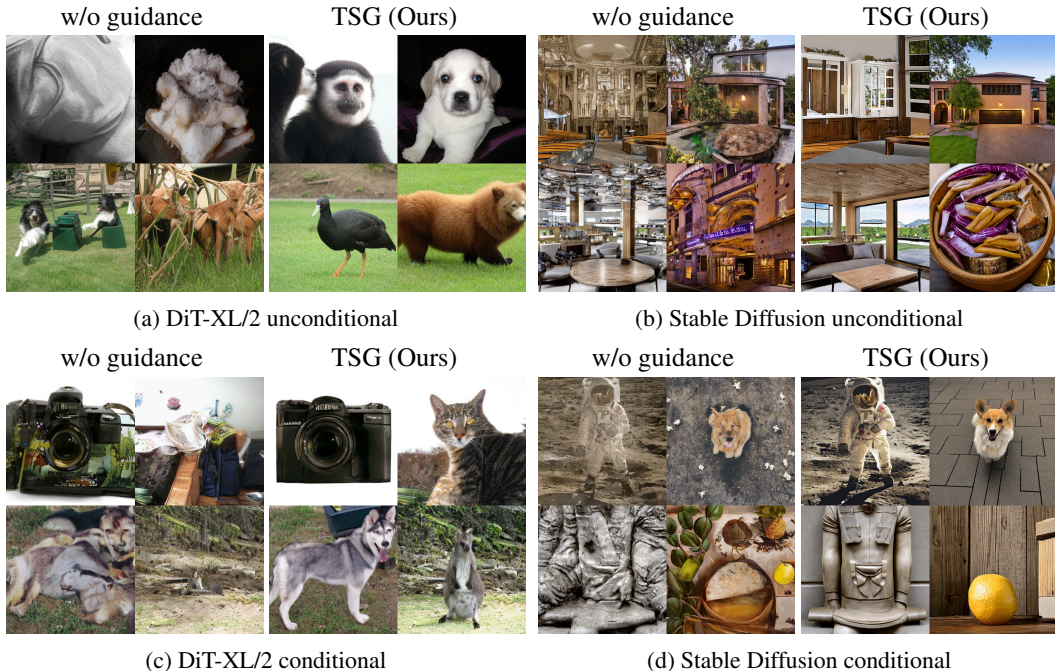


Figure 5: Effectiveness of TSG to improve the quality of both unconditional and conditional generation across two different models: DiT-XL/2 [29] for class-conditional generation, and Stable Diffusion [33] for text-conditional generation. Results are best seen when zoomed in.

Table 3: Quantitative comparison between the baseline sampling of the diffusion models and sampling with TSG. TSG significantly boosts quality (lower FID) across various setups.

Model	Architecture	Type	Guidance	FID ↓	Precision ↑	Recall ↑
Stable Diffusion [33]	UNet	Unconditional	✗	69.38	0.42	0.49
			TSG (Ours)	56.65	0.54	0.54
		Text-conditional	✗	36.63	0.48	0.64
			TSG (Ours)	22.17	0.62	0.59
DiT-XL/2 [29]	Transformer	Unconditional	✗	48.67	0.48	0.59
			TSG (Ours)	29.03	0.69	0.55
		Class-conditional	✗	15.49	0.64	0.74
			TSG (Ours)	6.39	0.82	0.65

6.3 Effectiveness of time-step guidance

Lastly, we show the effectiveness of time-step guidance in improving the quality of generation without relying on any information about the conditioning signal. The qualitative results are given in Figure 5. We can see that TSG increases the image quality of both conditional and unconditional sampling. Table 3 also presents the quantitative evaluation of TSG for both conditional and unconditional generation. Similar to CFG, using TSG significantly improves FID by trading diversity with quality. Finally, Figure 6 shows how TSG behaves as we increase the guidance scale. We observe that similar to CFG, TSG also has a U-shaped plot for the FID as the guidance scale increases.

7 Ablation studies

We next present the ablation studies on the effect of random conditioning in ICG and the hyperparameters in TSG. All ablations are conducted using the DiT-XL/2 model [29].

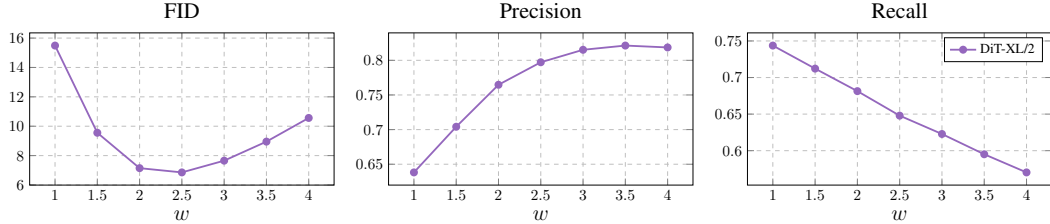


Figure 6: Effect of TSG as the guidance scale increases for DiT-XL/2 [29]. Similar to CFG, TSG also significantly improves FID by trading diversity (recall) with quality (precision).

Table 4: Ablation on the choice of independent condition in ICG.

ICG method	FID ↓	Precision ↑	Recall ↑
Gaussian noise	5.50	0.83	0.65
Random condition	5.55	0.83	0.65

Table 5: Ablation study examining various design elements in TSG.

(a) Influence of the noise scale s				(b) Influence of α				(c) Maximum layer index			
s	FID ↓	Precision ↑	Recall ↑	α	FID ↓	Precision ↑	Recall ↑	Index	FID ↓	Precision ↑	Recall ↑
1.0	10.23	0.69	0.35	0.75	7.22	0.82	0.62	5	7.84	0.75	0.69
2.0	6.85	0.80	0.69	1.0	6.39	0.84	0.65	10	6.85	0.79	0.65
2.5	7.94	0.80	0.69	1.25	6.47	0.78	0.66	15	7.65	0.82	0.65

The choice of random condition in ICG We first show that both Gaussian noise and random conditions can be used for estimating the unconditional part in ICG. The quantitative results are given in Table 4. The table shows that both methods are viable options for simulating classifier-free guidance without training.

Impact of hyperparameters in time-step guidance This ablation study explores the effect of hyperparameters in TSG. The results are presented in Table 5. We observe that as we introduce more perturbation into the time-step embedding of the model, in the form of higher noise scale s (Table 5a), lower power α (Table 5b), or higher layer index (Table 5c), precision improves while recall decreases. This suggests that the amount of perturbation should be balanced for a good trade-off between diversity and quality. We also empirically observed that adding too much noise to the time-step embedding hurts image quality.

8 Discussion and conclusion

In this paper, we revisited the core aspects of classifier-free guidance and showed that by replacing the conditional vector in a trained conditional diffusion model with an independent condition, we can efficiently estimate the score of the unconditional distribution. We then introduced independent condition guidance (ICG), a novel method that simulates the same behavior as CFG without the need to learn an unconditional model during training. Inspired by this, we also proposed time-step guidance (TSG) and demonstrated that the time-step information learned by the diffusion model can be leveraged to enhance the quality of generations, even for unconditional models. Our experiments showed that ICG performs similarly to standard CFG and alleviates the need to consider the CFG objective during training. Thus, ICG streamlines the training of conditional models and potentially improves the training efficiency. Additionally, we verified that TSG also improves generation quality in a manner similar to CFG, without relying on any conditional information. As with CFG, challenges remain in accelerating the proposed methods so that the sampling cost approaches that of an unguided sampling process (i.e., removing the need to query the diffusion network twice at each sampling step); we consider this topic as a promising avenue for further research.

References

- [1] Donghoon Ahn, Hyoungwon Cho, Jaewon Min, Wooseok Jang, Jungwoo Kim, Seonhwa Kim, Hyun Hee Park, Kyong Hwan Jin, and Seungryong Kim. Self-rectifying diffusion sampling with perturbed-attention guidance. *CoRR*, abs/2403.17377, 2024. doi: 10.48550/ARXIV.2403.17377. URL <https://doi.org/10.48550/arXiv.2403.17377>.
- [2] Yogesh Balaji, Seungjun Nah, Xun Huang, Arash Vahdat, Jiaming Song, Karsten Kreis, Miika Aittala, Timo Aila, Samuli Laine, Bryan Catanzaro, Tero Karras, and Ming-Yu Liu. ediff-i: Text-to-image diffusion models with an ensemble of expert denoisers. *CoRR*, abs/2211.01324, 2022. doi: 10.48550/arXiv.2211.01324. URL <https://doi.org/10.48550/arXiv.2211.01324>.
- [3] Arpit Bansal, Hong-Min Chu, Avi Schwarzschild, Soumyadip Sengupta, Micah Goldblum, Jonas Geiping, and Tom Goldstein. Universal guidance for diffusion models. In *Proceedings of the IEEE/CVF Conference on Computer Vision and Pattern Recognition*, pages 843–852, 2023.
- [4] Andreas Blattmann, Tim Dockhorn, Sumith Kulal, Daniel Mendelevitch, Maciej Kilian, Dominik Lorenz, Yam Levi, Zion English, Vikram Voleti, Adam Letts, Varun Jampani, and Robin Rombach. Stable video diffusion: Scaling latent video diffusion models to large datasets. *CoRR*, abs/2311.15127, 2023. doi: 10.48550/ARXIV.2311.15127. URL <https://doi.org/10.48550/arXiv.2311.15127>.
- [5] Andreas Blattmann, Robin Rombach, Huan Ling, Tim Dockhorn, Seung Wook Kim, Sanja Fidler, and Karsten Kreis. Align your latents: High-resolution video synthesis with latent diffusion models. In *Proceedings of the IEEE/CVF Conference on Computer Vision and Pattern Recognition*, pages 22563–22575, 2023.
- [6] Andrew Brock, Jeff Donahue, and Karen Simonyan. Large scale GAN training for high fidelity natural image synthesis. In *7th International Conference on Learning Representations, ICLR 2019, New Orleans, LA, USA, May 6-9, 2019*. OpenReview.net, 2019. URL <https://openreview.net/forum?id=B1xsqj09Fm>.
- [7] Nanxin Chen, Yu Zhang, Heiga Zen, Ron J. Weiss, Mohammad Norouzi, and William Chan. Wavegrad: Estimating gradients for waveform generation. In *9th International Conference on Learning Representations, ICLR 2021, Virtual Event, Austria, May 3-7, 2021*. OpenReview.net, 2021. URL <https://openreview.net/forum?id=NsMLjcFaO8O>.
- [8] Hyungjin Chung, Jeongsol Kim, Michael T Mccann, Marc L Klasky, and Jong Chul Ye. Diffusion posterior sampling for general noisy inverse problems. *arXiv preprint arXiv:2209.14687*, 2022.
- [9] Prafulla Dhariwal and Alexander Quinn Nichol. Diffusion models beat gans on image synthesis. In Marc’Aurelio Ranzato, Alina Beygelzimer, Yann N. Dauphin, Percy Liang, and Jennifer Wortman Vaughan, editors, *Advances in Neural Information Processing Systems 34: Annual Conference on Neural Information Processing Systems 2021, NeurIPS 2021, December 6-14, 2021, virtual*, pages 8780–8794, 2021. URL <https://proceedings.neurips.cc/paper/2021/hash/49ad23d1ec9fa4bd8d77d02681df5cfa-Abstract.html>.
- [10] Agrim Gupta, Lijun Yu, Kihyuk Sohn, Xiuye Gu, Meera Hahn, Li Fei-Fei, Irfan Essa, Lu Jiang, and José Lezama. Photorealistic video generation with diffusion models. *arXiv preprint arXiv:2312.06662*, 2023.
- [11] Yutong He, Naoki Murata, Chieh-Hsin Lai, Yuhta Takida, Toshimitsu Uesaka, Dongjun Kim, Wei-Hsiang Liao, Yuki Mitsufuji, J Zico Kolter, Ruslan Salakhutdinov, et al. Manifold preserving guided diffusion. *arXiv preprint arXiv:2311.16424*, 2023.
- [12] Martin Heusel, Hubert Ramsauer, Thomas Unterthiner, Bernhard Nessler, and Sepp Hochreiter. Gans trained by a two time-scale update rule converge to a local nash equilibrium. In Isabelle Guyon, Ulrike von Luxburg, Samy Bengio, Hanna M. Wallach, Rob Fergus, S. V. N. Vishwanathan, and Roman Garnett, editors, *Advances in Neural Information Processing Systems 30: Annual Conference on Neural Information Processing Systems 2017, December 4-9, 2017, Long Beach, CA, USA*, pages 6626–6637, 2017. URL <https://proceedings.neurips.cc/paper/2017/hash/8a1d694707eb0fefe65871369074926d-Abstract.html>.
- [13] Jonathan Ho and Tim Salimans. Classifier-free diffusion guidance. *CoRR*, abs/2207.12598, 2022. doi: 10.48550/arXiv.2207.12598. URL <https://doi.org/10.48550/arXiv.2207.12598>.

- [14] Jonathan Ho, Ajay Jain, and Pieter Abbeel. Denoising diffusion probabilistic models. In Hugo Larochelle, Marc’Aurelio Ranzato, Raia Hadsell, Maria-Florina Balcan, and Hsuan-Tien Lin, editors, *Advances in Neural Information Processing Systems 33: Annual Conference on Neural Information Processing Systems 2020, NeurIPS 2020, December 6-12, 2020, virtual*, 2020. URL <https://proceedings.neurips.cc/paper/2020/hash/4c5bcfec8584af0d967f1ab10179ca4b-Abstract.html>.
- [15] Susung Hong, Gyuseong Lee, Wooseok Jang, and Seungryong Kim. Improving sample quality of diffusion models using self-attention guidance. *CoRR*, abs/2210.00939, 2022. doi: 10.48550/arXiv.2210.00939. URL <https://doi.org/10.48550/arXiv.2210.00939>.
- [16] Emiel Hoogeboom, Jonathan Heek, and Tim Salimans. simple diffusion: End-to-end diffusion for high resolution images. *CoRR*, abs/2301.11093, 2023. doi: 10.48550/arXiv.2301.11093. URL <https://doi.org/10.48550/arXiv.2301.11093>.
- [17] Qingqing Huang, Daniel S. Park, Tao Wang, Timo I. Denk, Andy Ly, Nanxin Chen, Zhengdong Zhang, Zhishuai Zhang, Jiahui Yu, Christian Havnø Frank, Jesse H. Engel, Quoc V. Le, William Chan, and Wei Han. Noise2music: Text-conditioned music generation with diffusion models. *CoRR*, abs/2302.03917, 2023. doi: 10.48550/arXiv.2302.03917. URL <https://doi.org/10.48550/arXiv.2302.03917>.
- [18] Tero Karras, Miika Aittala, Timo Aila, and Samuli Laine. Elucidating the design space of diffusion-based generative models. 2022. URL <https://openreview.net/forum?id=k7FuTOWMOc7>.
- [19] Tero Karras, Miika Aittala, Jaakko Lehtinen, Janne Hellsten, Timo Aila, and Samuli Laine. Analyzing and improving the training dynamics of diffusion models, 2023.
- [20] Zhifeng Kong, Wei Ping, Jiaji Huang, Kexin Zhao, and Bryan Catanzaro. Diffwave: A versatile diffusion model for audio synthesis. In *9th International Conference on Learning Representations, ICLR 2021, Virtual Event, Austria, May 3-7, 2021*. OpenReview.net, 2021. URL <https://openreview.net/forum?id=a-xFK8Ymz5J>.
- [21] Tuomas Kynkäänniemi, Tero Karras, Samuli Laine, Jaakko Lehtinen, and Timo Aila. Improved precision and recall metric for assessing generative models. In Hanna M. Wallach, Hugo Larochelle, Alina Beygelzimer, Florence d’Alché-Buc, Emily B. Fox, and Roman Garnett, editors, *Advances in Neural Information Processing Systems 32: Annual Conference on Neural Information Processing Systems 2019, NeurIPS 2019, December 8-14, 2019, Vancouver, BC, Canada*, pages 3929–3938, 2019. URL <https://proceedings.neurips.cc/paper/2019/hash/0234c510bc6d908b28c70ff313743079-Abstract.html>.
- [22] Guan-Horng Liu, Arash Vahdat, De-An Huang, Evangelos A. Theodorou, Weili Nie, and Anima Anandkumar. I²sb: Image-to-image schrödinger bridge. *CoRR*, abs/2302.05872, 2023. doi: 10.48550/arXiv.2302.05872. URL <https://doi.org/10.48550/arXiv.2302.05872>.
- [23] Luping Liu, Yi Ren, Zhijie Lin, and Zhou Zhao. Pseudo numerical methods for diffusion models on manifolds. In *The Tenth International Conference on Learning Representations, ICLR 2022, Virtual Event, April 25-29, 2022*. OpenReview.net, 2022. URL <https://openreview.net/forum?id=PIKWVd2yBkY>.
- [24] Cheng Lu, Yuhao Zhou, Fan Bao, Jianfei Chen, Chongxuan Li, and Jun Zhu. Dpm-solver: A fast ODE solver for diffusion probabilistic model sampling in around 10 steps. In *NeurIPS*, 2022. URL http://papers.nips.cc/paper_files/paper/2022/hash/260a14acce2a89dad36adc8eefe7c59e-Abstract-Conference.html.
- [25] Cheng Lu, Yuhao Zhou, Fan Bao, Jianfei Chen, Chongxuan Li, and Jun Zhu. Dpm-solver++: Fast solver for guided sampling of diffusion probabilistic models. *CoRR*, abs/2211.01095, 2022. doi: 10.48550/arXiv.2211.01095. URL <https://doi.org/10.48550/arXiv.2211.01095>.
- [26] Kevin P. Murphy. *Probabilistic Machine Learning: Advanced Topics*. MIT Press, 2023. URL <http://probml.github.io/book2>.
- [27] Alexander Quinn Nichol and Prafulla Dhariwal. Improved denoising diffusion probabilistic models. In Marina Meila and Tong Zhang, editors, *Proceedings of the 38th International Conference on Machine Learning, ICML 2021, 18-24 July 2021, Virtual Event*, volume 139 of *Proceedings of Machine Learning Research*, pages 8162–8171. PMLR, 2021. URL <http://proceedings.mlr.press/v139/nichol21a.html>.

- [28] Alexander Quinn Nichol, Prafulla Dhariwal, Aditya Ramesh, Pranav Shyam, Pamela Mishkin, Bob McGrew, Ilya Sutskever, and Mark Chen. GLIDE: towards photorealistic image generation and editing with text-guided diffusion models. In Kamalika Chaudhuri, Stefanie Jegelka, Le Song, Csaba Szepesvári, Gang Niu, and Sivan Sabato, editors, *International Conference on Machine Learning, ICML 2022, 17-23 July 2022, Baltimore, Maryland, USA*, volume 162 of *Proceedings of Machine Learning Research*, pages 16784–16804. PMLR, 2022. URL <https://proceedings.mlr.press/v162/nichol22a.html>.
- [29] William Peebles and Saining Xie. Scalable diffusion models with transformers. *CoRR*, abs/2212.09748, 2022. doi: 10.48550/arXiv.2212.09748. URL <https://doi.org/10.48550/arXiv.2212.09748>.
- [30] Dustin Podell, Zion English, Kyle Lacey, Andreas Blattmann, Tim Dockhorn, Jonas Müller, Joe Penna, and Robin Rombach. SDXL: improving latent diffusion models for high-resolution image synthesis. *CoRR*, abs/2307.01952, 2023. doi: 10.48550/ARXIV.2307.01952. URL <https://doi.org/10.48550/arXiv.2307.01952>.
- [31] Ben Poole, Ajay Jain, Jonathan T. Barron, and Ben Mildenhall. Dreamfusion: Text-to-3d using 2d diffusion. In *The Eleventh International Conference on Learning Representations, ICLR 2023, Kigali, Rwanda, May 1-5, 2023*. OpenReview.net, 2023. URL <https://openreview.net/pdf?id=FjNys5c7VyY>.
- [32] Aditya Ramesh, Prafulla Dhariwal, Alex Nichol, Casey Chu, and Mark Chen. Hierarchical text-conditional image generation with CLIP latents. *CoRR*, abs/2204.06125, 2022. doi: 10.48550/arXiv.2204.06125. URL <https://doi.org/10.48550/arXiv.2204.06125>.
- [33] Robin Rombach, Andreas Blattmann, Dominik Lorenz, Patrick Esser, and Björn Ommer. High-resolution image synthesis with latent diffusion models. In *IEEE/CVF Conference on Computer Vision and Pattern Recognition, CVPR 2022, New Orleans, LA, USA, June 18-24, 2022*, pages 10674–10685. IEEE, 2022. doi: 10.1109/CVPR52688.2022.01042. URL <https://doi.org/10.1109/CVPR52688.2022.01042>.
- [34] Negar Rostamzadeh, Emily Denton, and Linda Petrini. Ethics and creativity in computer vision. *CoRR*, abs/2112.03111, 2021. URL <https://arxiv.org/abs/2112.03111>.
- [35] Seyedmorteza Sadat, Jakob Buhmann, Derek Bradley, Otmar Hilliges, and Romann M. Weber. CADs: Unleashing the diversity of diffusion models through condition-annealed sampling. In *The Twelfth International Conference on Learning Representations*, 2024. URL <https://openreview.net/forum?id=zMoNrajK2X>.
- [36] Chitwan Saharia, William Chan, Huiwen Chang, Chris A. Lee, Jonathan Ho, Tim Salimans, David J. Fleet, and Mohammad Norouzi. Palette: Image-to-image diffusion models. In Munkhtsetseg Nandigjav, Niloy J. Mitra, and Aaron Hertzmann, editors, *SIGGRAPH '22: Special Interest Group on Computer Graphics and Interactive Techniques Conference, Vancouver, BC, Canada, August 7 - 11, 2022*, pages 15:1–15:10. ACM, 2022. doi: 10.1145/3528233.3530757. URL <https://doi.org/10.1145/3528233.3530757>.
- [37] Chitwan Saharia, William Chan, Saurabh Saxena, Lala Li, Jay Whang, Emily L. Denton, Seyed Kamyar Seyed Ghasemipour, Raphael Gontijo Lopes, Burcu Karagol Ayan, Tim Salimans, Jonathan Ho, David J. Fleet, and Mohammad Norouzi. Photorealistic text-to-image diffusion models with deep language understanding. 2022. URL http://papers.nips.cc/paper_files/paper/2022/hash/ec795aeadae0b7d230fa35cbaf04c041-Abstract-Conference.html.
- [38] Tim Salimans and Jonathan Ho. Progressive distillation for fast sampling of diffusion models. In *The Tenth International Conference on Learning Representations, ICLR 2022, Virtual Event, April 25-29, 2022*. OpenReview.net, 2022. URL <https://openreview.net/forum?id=TIIdIXlpzhoI>.
- [39] Jascha Sohl-Dickstein, Eric A. Weiss, Niru Maheswaranathan, and Surya Ganguli. Deep unsupervised learning using nonequilibrium thermodynamics. 37:2256–2265, 2015. URL <http://proceedings.mlr.press/v37/sohl-dickstein15.html>.
- [40] Jiaming Song, Chenlin Meng, and Stefano Ermon. Denoising diffusion implicit models. In *9th International Conference on Learning Representations, ICLR 2021, Virtual Event, Austria, May 3-7, 2021*. OpenReview.net, 2021. URL <https://openreview.net/forum?id=StIgiarCHLP>.
- [41] Jiaming Song, Qinsheng Zhang, Hongxu Yin, Morteza Mardani, Ming-Yu Liu, Jan Kautz, Yongxin Chen, and Arash Vahdat. Loss-guided diffusion models for plug-and-play controllable

- generation. In *International Conference on Machine Learning*, pages 32483–32498. PMLR, 2023.
- [42] Yang Song and Stefano Ermon. Generative modeling by estimating gradients of the data distribution. In Hanna M. Wallach, Hugo Larochelle, Alina Beygelzimer, Florence d’Alché-Buc, Emily B. Fox, and Roman Garnett, editors, *Advances in Neural Information Processing Systems 32: Annual Conference on Neural Information Processing Systems 2019, NeurIPS 2019, December 8-14, 2019, Vancouver, BC, Canada*, pages 11895–11907, 2019. URL <https://proceedings.neurips.cc/paper/2019/hash/3001ef257407d5a371a96dcd947c7d93-Abstract.html>.
- [43] Yang Song, Jascha Sohl-Dickstein, Diederik P. Kingma, Abhishek Kumar, Stefano Ermon, and Ben Poole. Score-based generative modeling through stochastic differential equations. In *9th International Conference on Learning Representations, ICLR 2021, Virtual Event, Austria, May 3-7, 2021*. OpenReview.net, 2021. URL <https://openreview.net/forum?id=PXTIG12RRHS>.
- [44] George Stein, Jesse Cresswell, Rasa Hosseinzadeh, Yi Sui, Brendan Ross, Valentin Vilecroze, Zhaoyan Liu, Anthony L Caterini, Eric Taylor, and Gabriel Loaiza-Ganem. Exposing flaws of generative model evaluation metrics and their unfair treatment of diffusion models. *Advances in Neural Information Processing Systems*, 36, 2024.
- [45] Guy Tevet, Sigal Raab, Brian Gordon, Yonatan Shafir, Daniel Cohen-Or, and Amit Haim Bermano. Human motion diffusion model. 2023. URL <https://openreview.net/pdf?id=SJ1kSyO2jwu>.
- [46] Jonathan Tseng, Rodrigo Castellon, and C. Karen Liu. EDGE: editable dance generation from music. In *IEEE/CVF Conference on Computer Vision and Pattern Recognition, CVPR 2023, Vancouver, BC, Canada, June 17-24, 2023*, pages 448–458. IEEE, 2023. doi: 10.1109/CVPR52729.2023.00051. URL <https://doi.org/10.1109/CVPR52729.2023.00051>.
- [47] Jiahui Yu, Yuanzhong Xu, Jing Yu Koh, Thang Luong, Gunjan Baid, Zirui Wang, Vijay Vasudevan, Alexander Ku, Yinfei Yang, Burcu Karagol Ayan, Ben Hutchinson, Wei Han, Zarana Parekh, Xin Li, Han Zhang, Jason Baldridge, and Yonghui Wu. Scaling autoregressive models for content-rich text-to-image generation. *Trans. Mach. Learn. Res.*, 2022, 2022. URL <https://openreview.net/forum?id=AFDcYJKhND>.
- [48] Jiwen Yu, Yinhuai Wang, Chen Zhao, Bernard Ghanem, and Jian Zhang. Freedom: Training-free energy-guided conditional diffusion model. In *Proceedings of the IEEE/CVF International Conference on Computer Vision*, pages 23174–23184, 2023.

A Broader impact statement

As generative modeling advances, the creation and spread of fabricated or inaccurate data become easier. Thus, while improvements in AI-generated content can boost productivity and creativity, it is crucial to carefully consider the associated risks and ethical implications. For a more detailed discussion on the ethics and creativity in computer vision, we refer readers to [34].

B Intuition behind TSG

This section demonstrates that if we perturb the time step with a positive or negative constant (using $t + \delta$ or $t - \delta$) to guide the sampling, it results in insufficient or excessive noise removal. As shown in Figure 7, using lower time steps causes the model to perform excessive noise removal (soft outputs), while using higher time steps forces the model to perform insufficient noise removal (noisy images). TSG uses both directions to prevent the outputs from moving toward these undesirable paths, thereby increasing the quality of the generations.

C More experiments

This section includes additional experiments on ICG and TSG. Experiments in this section are conducted based on the DiT-XL/2 model [29].

C.1 Compatibility of ICG with CADS

We show that ICG is compatible with CADS [35], and CADS can be used on top of ICG to increase the diversity of generations. An example of applying CADS to ICG is shown in Figure 8, and the quantitative results are given in Table 6 for the DiT-XL/2 model. As ICG behaves similarly to the standard CFG, applying CADS increases diversity with minimal drop in quality.

Table 6: Effectiveness of CADS on ICG.

Guidance	FID ↓	Precision ↑	Recall ↑
ICG	20.56	0.89	0.32
+CADS	8.83	0.78	0.61

C.2 Combining TSG and ICG

We next demonstrate that ICG and TSG can be complementary to each other when combined at the proper scale. The quantitative results of this experiment are presented in Table 7 with a visual example given in Figure 9. The table indicates that the combination of ICG and TSG outperforms each method in isolation in terms of FID, and all guided sampling algorithms significantly outperform the non-guided baseline.

D Implementation details

The sampling details for ICG and TSG are provided in Algorithms 1 and 2. Both algorithms are straightforward to implement and require minimal code changes compared to the base sampling. The pseudocode for implementing ICG and TSG is also included in Figures 10 and 11. Additionally, the hyperparameters used in our experiments are listed in Tables 8 and 9. The CADS experiment was conducted with a linear schedule using $\tau_1 = 0.5$, $\tau_2 = 0.9$, and $s_{\text{CADS}} = 0.15$. Lastly, please note that we did not perform an exhaustive grid search on the parameters of TSG, and better configurations are likely to exist for each model.

For the TSG noise schedule, we experimented with a constant and a power schedule, as shown in Figure 11, and found that both work similarly. We recommend using the power schedule as it offers more flexibility over the scale of the noise at each t . The constant schedule is technically a special case of the power schedule where the exponent is zero. We also found it useful to apply TSG only at intervals during the sampling, i.e., for $t \in [T_{\min}, T_{\max}]$, where T_{\min} and T_{\max} are hyperparameters. Also, when limiting TSG to only a portion of layers in the diffusion model, we used the first N layers of transformer-based architectures and the first N layers of the encoder and decoder in UNet-based

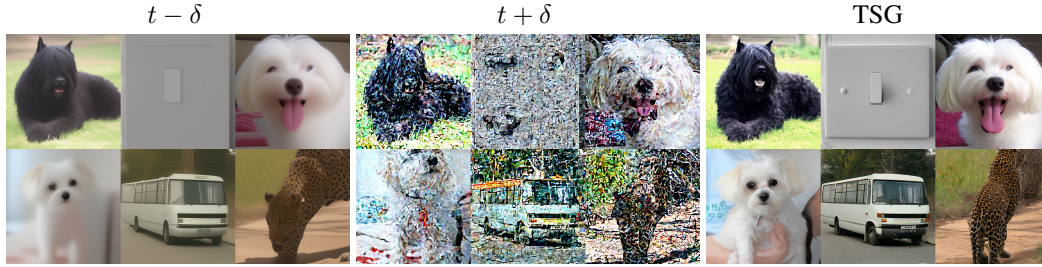


Figure 7: Intuition behind TSG: Using lower time steps for guidance causes excessive noise removal (soft outputs), while higher time steps cause insufficient noise removal (noisy images). TSG employs both directions to improve output quality.

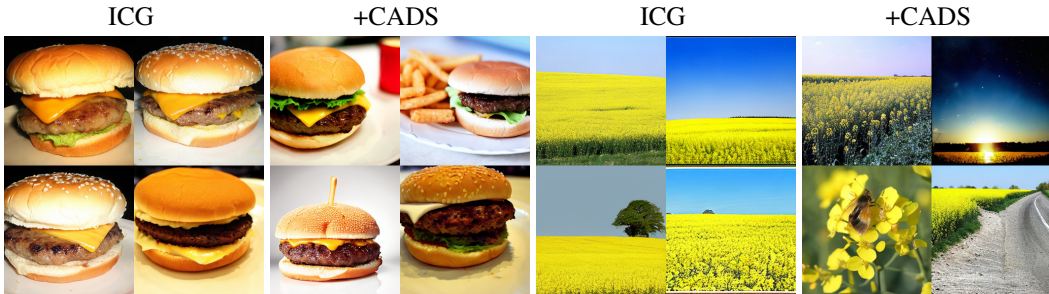


Figure 8: Similar to CFG, ICG is compatible with CADS, and CADS can be used to increase the diversity of ICG at higher guidance scales. Samples are generated from the DiT-XL/2 model.



Figure 9: Visual example of combining ICG and TSG. The combination provides better visual generations compared to the baseline and only ICG.

Table 7: Compatibility of ICG and TSG. Applying both guidance methods gives the best FID.

ICG	TSG	FID ↓	Precision ↑	Recall ↑
✗	✗	15.49	0.64	0.74
✓	✗	6.47	0.77	0.69
✗	✓	9.55	0.70	0.71
✓	✓	5.76	0.82	0.65

architectures. We chose to scale the amount of noise s based on the standard deviation of the time-step embedding (see Figures 10 and 11) for more fine-grained control over the scale.

E More visual results

This section presents additional visual results for our guidance methods. More results on ICG are provided in Figure 12, while additional results for TSG are shown in Figures 13 and 14. Consistent with the main results of the paper, ICG produces similar outcomes to CFG, and TSG consistently enhances the quality compared to the baseline. Finally, Figure 15 provides examples of the effectiveness of TSG based on the Stable Diffusion XL (SDXL) model [30].

Algorithm 1 Sampling with ICG

Require: w_{ICG} : ICG strength**Require:** \mathbf{y} : Input condition1: Initial value: $\mathbf{z}_1 \sim \mathcal{N}(\mathbf{0}, \mathbf{I})$ 2: **for** $t = T, \dots, 1$ **do**3: ◦ Pick a random $\hat{\mathbf{y}}$ independent of the input (Gaussian noise or from the conditioning space).4: ◦ Compute the ICG guided output at t :

$$\hat{D}_{\text{ICG}}(\mathbf{z}_t, t, \mathbf{y}) = D(\mathbf{z}_t, t, \hat{\mathbf{y}}) + w_{\text{ICG}}(D(\mathbf{z}_t, t, \mathbf{y}) - D(\mathbf{z}_t, t, \hat{\mathbf{y}})).$$

5: ◦ Perform one sampling step (e.g. one step of DDPM):

$$\mathbf{z}_{t-1} = \text{diffusion_reverse}(\hat{D}_{\text{ICG}}, \mathbf{z}_t, t).$$

6: **end for**7: **return** \mathbf{z}_0

Algorithm 2 Sampling with TSG

Require: w_{TSG} : TSG strength**Require:** (s, α) : TSG hyperparameters**Require:** \mathbf{y} : Input condition (optional)1: Initial value: $\mathbf{z}_1 \sim \mathcal{N}(\mathbf{0}, \mathbf{I})$ 2: **for** $t = T, \dots, 1$ **do**3: ◦ Perturb the time-step embedding t_{emb} to get \tilde{t}_{emb} , i.e., set $\tilde{t}_{\text{emb}} = t_{\text{emb}} + st^\alpha \mathbf{n}$.4: ◦ Compute the TSG guided output at t :

$$\hat{D}_{\text{TSG}}(\mathbf{z}_t, t, \mathbf{y}) = D(\mathbf{z}_t, \tilde{t}_{\text{emb}}, \mathbf{y}) + w_{\text{TSG}}(D(\mathbf{z}_t, t_{\text{emb}}, \mathbf{y}) - D(\mathbf{z}_t, \tilde{t}_{\text{emb}}, \mathbf{y})).$$

5: ◦ Perform one sampling step (e.g. one step of DDPM):

$$\mathbf{z}_{t-1} = \text{diffusion_reverse}(\hat{D}_{\text{TSG}}, \mathbf{z}_t, t).$$

6: **end for**7: **return** \mathbf{z}_0

Table 8: Hyperparameters used for the ICG experiments.

Model	ICG mode	ICG scale	CFG scale
DiT-XL/2	Random class	1.4	1.5
Stable Diffusion	Random text	3.0	4.0
Pose-to-Image	Gaussian noise	3.0	4.0
MDM	Gaussian noise	2.5	2.5
EDM	Random class	1.05	1.1
EDM2	Random class	1.25	1.25

Table 9: Hyperparameters used for the TSG experiments.

Model	Mode	TSG function	TSG scale	TSG parameters
DiT-XL/2	Unconditional	constant_schedule	5.0	T_MIN = 200, T_MAX = 800, $s = 1.0$
DiT-XL/2	Conditional	power_schedule	2.5	T_MIN = 0, T_MAX = 1000, $\alpha = 1, s = 2$
Stable Diffusion	Unconditional	constant_schedule	3.0	T_MIN = 100, T_MAX = 900, $s = 1.25$
Stable Diffusion	Conditional	power_schedule	4.0	T_MIN = 400, T_MAX = 1000, $s = 3.0, \alpha = 0.25$

```

1 def get_random_class():
2     """Random class labels."""
3     y_random = torch.randint(0, NUM_CLASSES, (BATCH_SIZE, ))
4     return y_random
5
6 def get_random_text():
7     """Random text tokens."""
8     random_idx = torch.randint(0, NUM_TOKENS, (BATCH_SIZE, MAX_LENGTH))
9     random_tokens = text_encoder(random_idx, attention_mask=None)[0]
10    return random_tokens
11
12 def get_gaussian_noise_embedding(embeddings):
13    """Random embedding based on Gaussian noise."""
14    noise_embedding = torch.randn_like(embeddings) * embeddings.std()
15    return noise_embedding
16
17 def get_gaussian_noise_image(image_cond):
18    """Random condition for image-conditional models (e.g., pose-to-image)."""
19    noise_embedding = torch.randn_like(image_cond) * SCALE
20    return noise_embedding
21

```

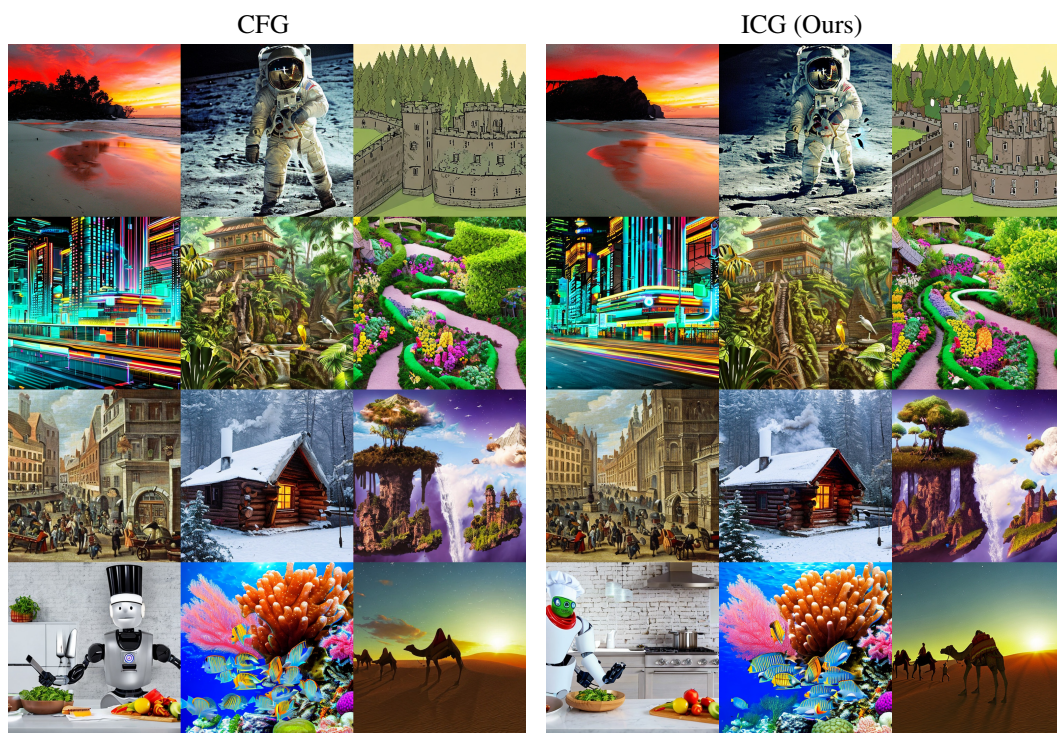
Figure 10: Implementation details for ICG. The figure presents pseudocode for implementing the random class, random text, and Gaussian noise embedding for the unconditional component in ICG.

```

1 def get_constant_schedule(t_emb, t, std_scaling=True):
2     """Applies TSG for a portion of sampling (t in [T_MIN, T_MAX])."""
3     if t < T_MIN or t > T_MAX:
4         return t_emb
5     noise_scale = S
6     if std_scaling:
7         noise_scale = S * t_emb.std()
8     that_emb = t_emb + torch.randn_like(t_emb) * noise_scale
9     return that_emb
10
11
12 def get_power_schedule(t_emb, t, std_scaling=True):
13    """Applies TSG according to the power schedule."""
14    if t < T_MIN or t > T_MAX:
15        return t_emb
16    noise_scale = S * t ** (ALPHA)
17    if std_scaling:
18        noise_scale = noise_scale * t_emb.std()
19    that_emb = t_emb + torch.randn_like(t_emb) * noise_scale
20    return that_emb
21

```

Figure 11: Implementation details for TSG. We provide two scheduling techniques for perturbing the time-step embedding. We empirically found that both methods perform similarly.



(a) Stable Diffusion

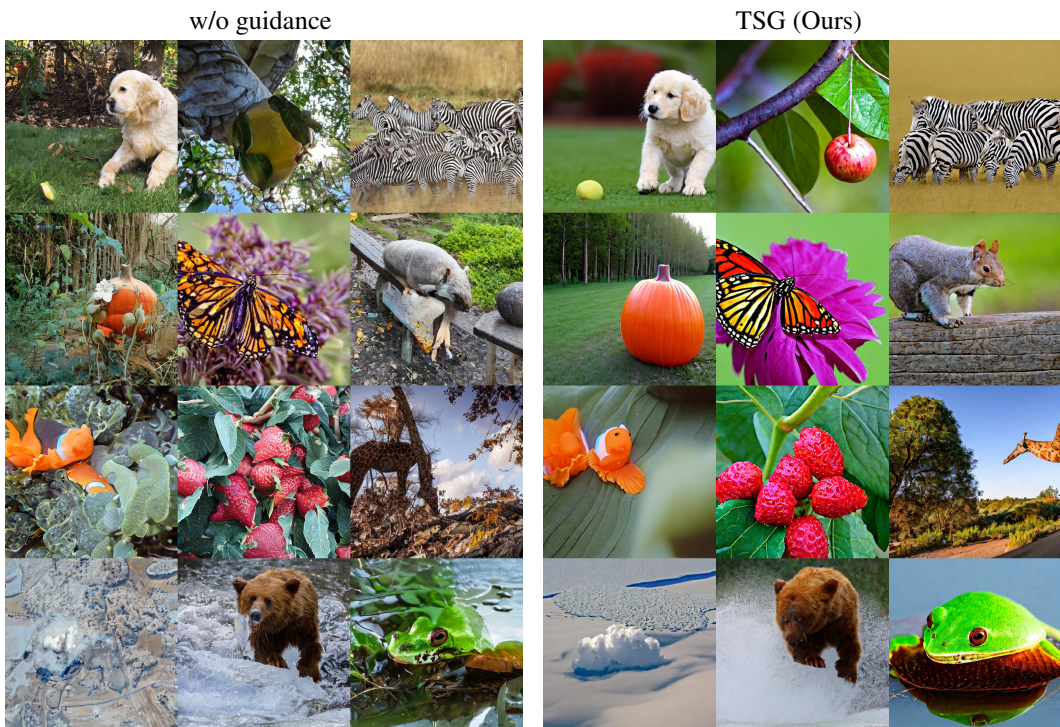


(b) DiT-XL/2

Figure 12: More comparisons between ICG and CFG for (a) text-to-image generation with Stable Diffusion [33] and (b) class-conditional generation with DiT-XL/2 [29].

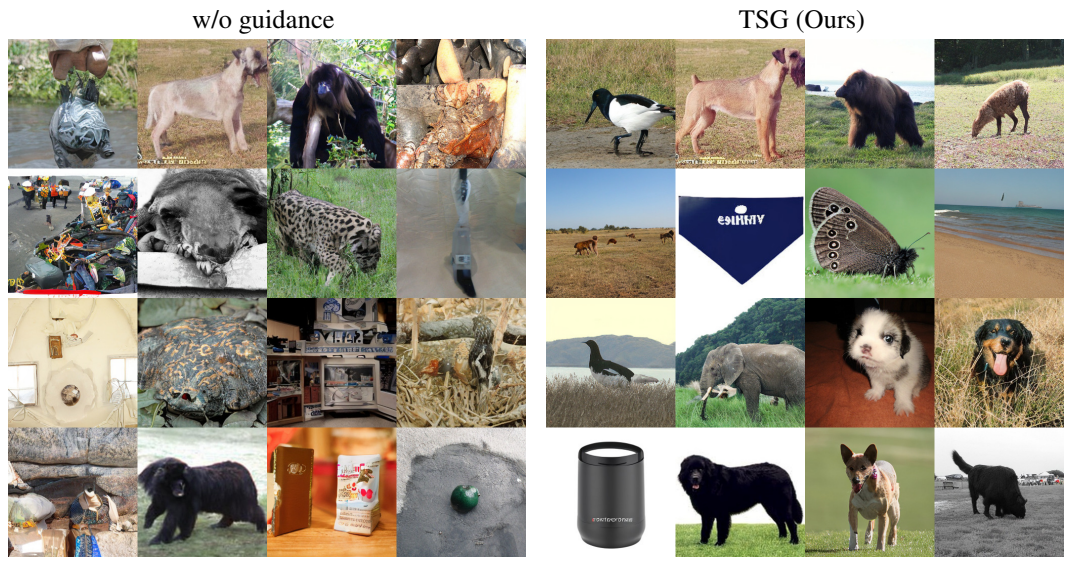


(a) Stable Diffusion unconditional

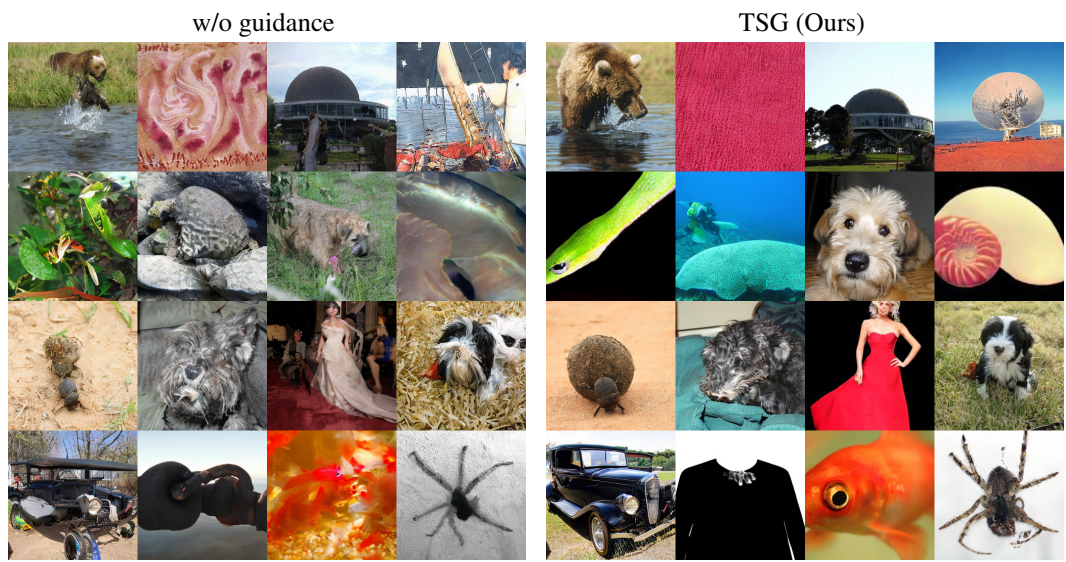


(b) Stable Diffusion conditional

Figure 13: More comparisons on the effectiveness of TSG for improving the quality of both unconditional and conditional generation for Stable Diffusion [33].



(a) DiT-XL/2 unconditional



(b) DiT-XL/2 conditional

Figure 14: More comparisons on the effectiveness of TSG for improving the quality of both unconditional and conditional generation for DiT-XL/2 [29].

"A photorealistic image of a car"



"A golden retriever puppy"



"A photorealistic image of a piano"



Figure 15: Showcasing the effectiveness of TSG in improving the quality of generations compared to sampling without guidance based on the SDXL model [30].